PERFORMANCE OF THE PHENIX EM CALORIMETER

G. David, E. Kistenev, A. Patwa, S. Stoll, S. White and C. Woody
Brookhaven National Laboratory, Upton, NY 11973, USA

S. Belikov, A. Denisov, Yu. Gilitzky, V. Kochetkov,
Y. Melnikov, Y. Mikhailov, V. Onuchin and V. Semenov
Institute of High Energy Physics, Protvino, Russia

Abstract

The PHENIX Electromagnetic Calorimeter is a large 15,552 channel lead/scintillator sampling calorimeter based on the shish-kebab optical readout technique. In this report we summarize studies leading to an optimal design for measurement of photons and electrons in the 1 GeV momentum range within the high multiplicity environment expected for events at RHIC. Timing resolutions of $\sim$ 100 ps and a sampling dominated energy resolution of 8% at 1 GeV are featured. We also present a novel scheme for monitoring gain and timing of our entire system.

Test results with a 144 channel preproduction "super-module" exposed to electron and hadron beams at the AGS are described. The calorimeter is currently under construction in Russia and the US and will be installed at RHIC during 1998.

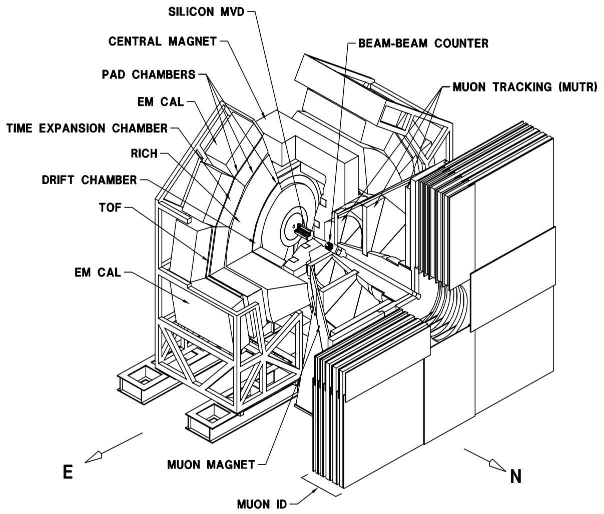

Figure 1: Cutaway view of the PHENIX Experimental layout.

I. Requirements

The central spectrometer of the PHENIX Experiment at RHIC is constructed from two Arms, each subtending a band of $\pm 20°$ about the perpendicular to the beam directions and 90° in azimuth. Outside of the charged particle tracking regions, the electromagnetic calorimeter walls are located 5.3m from the RHIC colliding beams (Figure 1).

The calorimeter will measure photons and electrons produced in Heavy Ion collisions (where charged multiplicities of up to $\sim$ 350 over the calorimeter area are expected). The long flight path to the calorimeter allows for some charged particle identification by time-of-flight (tof) since $\pi^{\pm}(K^{\pm})$ (with an average momenta of p_t= 300 MeV/c) lag behind the "photon flash" by 2(16) nsec. The calorimeter timing measurement complements that of the limited size, high precision TOF scintillator hodoscope. In addition, it provides the only means of measuring the tof of $\bar{n}$'s and other potential neutral backgrounds to γ's.

II. Construction

The basic calorimeter element is a module consisting of 4 electromagnetic towers with transverse dimensions of 5.5 cm (Figure 2). It consists of 66 layers of alternating Pb (1.5 mm thick) absorber plates, Tyvek optical reflector paper and 4 quadrants of scintillator plates (4 mm thick). The scintillator plates are produced by injection molding from a dry mix of Polystyene, Para-terphenyl and POPOP. The module is assembled on a fixture which provides mechanical training of the stack and then the module is tack welded in compression with 0.1 mm thick side straps. End pieces are formed from injection molded plastic with a thin steel shell.

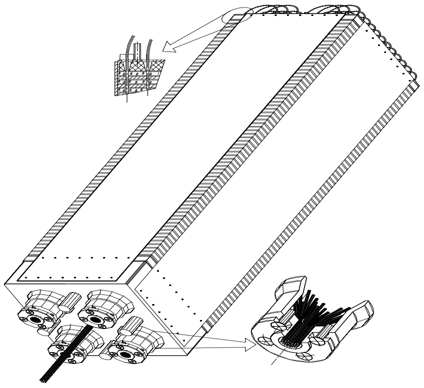

Figure 2: Four tower module assembly.

The scintillator plates are optically isolated from one another with an aluminization layer along their edges. The central corner of each scintillator has a window from which the aluminization is excluded. A source of UV can then be passed through a 3mm diameter hole down the center of the module and excite the scintillator for monitoring purposes.

III. Readout Principle

Scintillation light produced in the tower is read out through waveshifter doped polystyrene fibers which penetrate the module. A total of 36 fiber penetrations are provided in each tower as part of the scintillator mold. A single, continuous fiber is looped through 2 penetrations so that light emitted in both directions in the fiber will reach the readout end. This increases the size of the light signal and reduces the effect of attenuation in the fiber by a factor of 2. The fiber ends are compressed in a collet, hand polished and phototubes are mounted on the ends with an air gap.

A. *Optimization*

The PHENIX group carried out an R&D program to optimize the parameters of the optical system with respect to photostatistics, uniformity and speed of the calorimeter. A photomultiplier was developed in Russia for the project with a $\sim 16\%$ typical quantum efficiency at the emission maximum wavelength of the calorimeter (490 nm) and risetime of 5ns. Test results have been described elsewhere [2].

Among the scintillator plates which we tested were cast PVT based scintillator (BC404) with holes drilled for the fiber channels and a variety of injection molded PS based tiles. Different mixtures of primary scintillator (p-terphenyl) and secondary scintillator (POPOP) were tested for light yield and an optimum of 1.75% : 0.01% was chosen. A summary of

PT (%)	PPO (%)	POPOP (%)	BF203 (%)	I_{mean} BCF99-29A
1.0			0.01	65.7
1.5			0.02	68.0
1.5			0.03	78.7
1.5			0.05	82.2
2.0		0.005		86.9
1.0		0.01		75.5
1.5		0.01		81.5
1.75		0.01		92.9
2.0		0.01		79.6
2.5		0.01		80.2
1.0		0.03		70.2
1.5		0.03		72.4
1.75		0.03		80.0
1.0		0.05		58.6
1.5		0.05		82.6
1.75		0.05		87.2
1.5		0.1		86.4
	1.5	0.01		82.1
	1.75	0.01		84.9
	2.0	0.01		83.2

Figure 3: Light yield (arbitrary units) vs. scintillator composition when read out with BCF99-29A waveshifter fibers.

measured light yields is presented in Figure 3. BF203 is a Bicron fluor whose emission spectrum is better matched to the G2 waveshifter used in our readout fibers than that of POPOP.

We selected a waveshifter fluor with a fast (2.8 nsec) decay constant and a 407 nm peak absorption wavelength. The concentration was optimised using a series of fibers provided by Bicron Corp [1] and testing for effective attenuation length (which decreases with concentration).

Fiber	BCF92	BCF99-29a	BCF99-29b	R26	K27
Diameter (mm)	1 and 1.2	1	1	1.2	1.2
Core	PS	–	–	PS	PS
ref. index	1.59	–	–	1.59	1.59
Cladding					
inner	PMMA	–	–	PMMA	PMMA
ref.ind.	1.49	–	–	1.49	1.49
outer	-	-	-	Fluorine	polymer
ref.ind.				1.42	1.42
Fluor	G2, x mg/l	G2, 2x mg/l	G2, 4x mg/l	R26	K27
Num. aperture (%)	3.54	–	–	6	6
Peak Abs. (nm)	407	–	–	450	400-460
Peak Emis. (nm)	492	–	–	530	490
Decay time (ns)	2.8	–	–	11	6.7
L_{att} (m)	3.1	2.7	2.1	2.5	2

Figure 4: Characteristics of WLS fibers tested.

Tyvek and other reflector materials were tested for spectral reflectance in the wavelength region of 300nm to 600nm and Dupont 1055B, which was finally selected, was found to give approximately 50% higher light yield than white paper.

IV. Monitoring Scheme

Gain monitoring of the calorimeter will be based on a UV light pulse delivery system which couples to a leaky fiber that illuminates all scintillator tiles in a module (Figure 5). A prototype of this system has been operated at the AGS for over 6 months. The laser calibration was used to check gain stability and also provided a link between calibration runs and beam data taking.

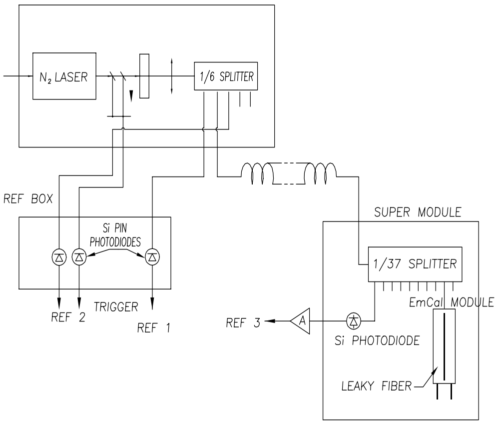

Figure 5: Laser monitoring scheme used for the AGS testbeam run.

V. Testbeam Results

A preproduction supermodule consisting of a 6×6 module array (144 towers total) was assembled at the end of 1994 and installed at the Brookhaven AGS testbeam for the Spring '95 run. Our testbeam measurements emphasized the low energy response of the calorimeter and timing resolution with electrons and hadrons over the range $0.3 \leq p \leq 7$ GeV/c.

The initial calibration of the calorimeter channels was obtained with cosmic ray muons selected prior to accelerator startup. A typical cosmic ray event is shown in Figure 6, in which the full supermodule is traversed by a muon track transverse to the tower axis. We are designing the calorimeter electronics to provide an internal majority trigger based on the number of towers above threshold in a supermodule. The most probable energy deposit is 42 MeV/tower. Calibration obtained from the muon peaks agreed to within 5% of that obtained from a 1 GeV electron beam.

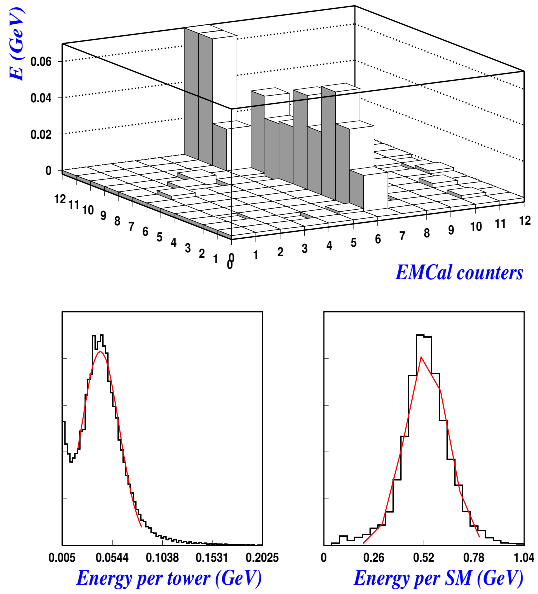

Figure 6: Response to cosmic ray muons traversing the calorimeter- a single event lego plot and the distribution of single channel and channel sums.

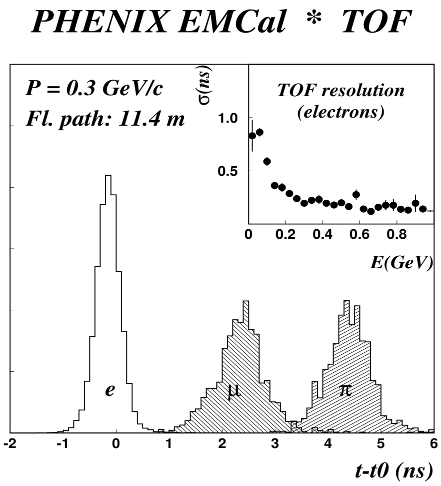

Figure 7: Time-of-flight resolution for electromagnetic showers vs. energy deposit. The lower figure shows the timing channel line shapes for a 300MeV/c beam.

A. *Time resolution*

We used leading edge discriminators to derive timing signals from the calorimeter PMT's and corrected offline for pulse height slewing. Figure 7 shows the arrival time distribution measured for 300 Mev/c electrons, muons and pions relative to a scintillation counter placed 11m upstream in the testbeam (twice the flight path in PHENIX). The timing resolution is 100 psec at 1 GeV/c for electromagnetic showers and worsens at lower energy due to photostatistics (the calorimeter light yield corresponds to $\geq$ 1600 p.e. per GeV).

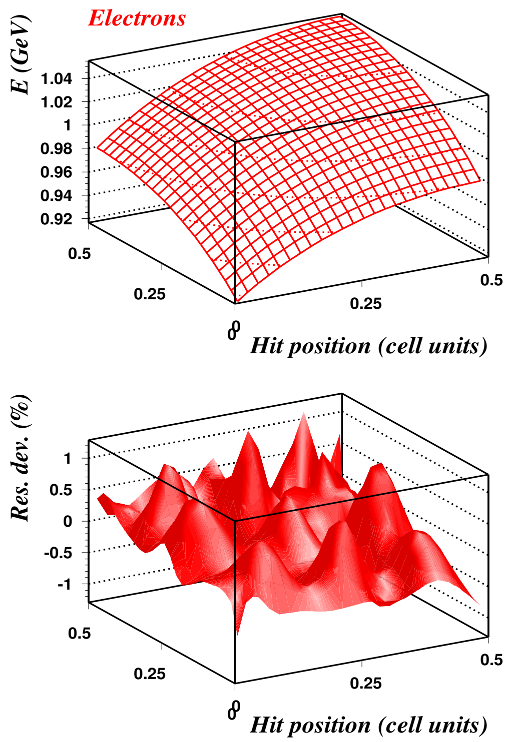

Figure 8: EMCal Uniformity Scan of electrons.

B. *Response Uniformity and Energy Resolution*

The response uniformity and energy resolution of the calorimeter were measured in an electron beam while recording the impact point of tracks with a beamline tracking system. The variation of light yield in individual scintillators with aluminized edges was measured to be 8% at an edge relative to the center and somewhat larger to a corner. This variation was used to predict the amplitude variation for electromagnetic showers taking into account dead material as a function of impact point in the calorimeter. The calculated overall response map agrees well with a smooth fit to the data shown in the upper half of Figure 8. The response map can then be used to correct calorimeter pulse height as a funtion of shower impact so long as the impact can be determined from an external tracking device or from the position resolution of the calorimeter itself (which we measure to be $\frac{1.0cm}{\sqrt{E(GeV)}}$).

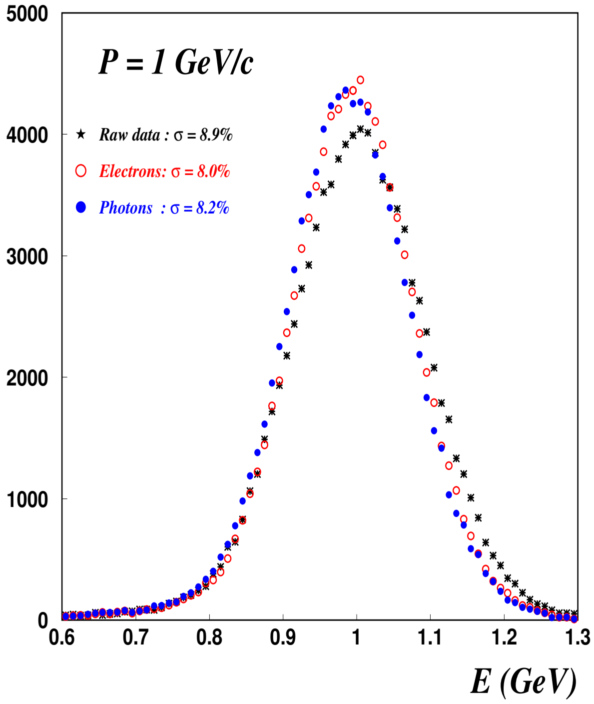

Figure 9: Energy resolution correction for Response Variations.

As shown in Figure 9, the raw energy resolution of 8.9% at 1 GeV decreases to 8.0% for electrons whose position will be determined by the tracking system. If there is no tracking information (i.e. as is the case for photon showers) then the resolution worsens to 8.2%. Using a detailed scan of the calorimeter response we have also been able to look for deviations from the simple smooth fit to calorimeter response variations which we use in our correction map. The lower half of Figure 8 shows that these deviations are of the order 1% or less and correspond to the fiber penetration pattern.

VI. Acknowledgements

We wish to thank the AGS staff and particularly our liaison engineer Dave Dayton for excellent support during our test. We also thank Bo Yu and David Whitehouse for assistance at various stages of data taking.

The authors also acknowledge the support of the US Department of Energy under contract DE-ACO2-76CH00016.

References

[1] BCF99-29a denotes a concentration of 2 times that of the product BCF92. Bicron Corp. Newburry, Ohio.

[2] G.David et al. IEEE Trans. on Nuclear Sci. 42, No.4, P.306 (1995). The 30 mm diameter FEU 115M 12-stage PMT was produced at Moscow Electric Light Plant (MELS), Moscow, Russia.